Determination of radial matrix elements and phase shifts in photoemission with a rotatable electric-field vector

Mathias Getzlaff, Matthias Bode, and Roland Wiesendanger
University of Hamburg, Institute of Applied Physics and Microstructure Research Center, Jungiusstrasse 11, D-20355 Hamburg, Germany
(Received 23 February 1998)

The electronic structure of hydrogen-adsorbate-induced states on Gd(0001) was investigated by means of photoelectron spectroscopy with linearly polarized radiation. Clean and well-ordered rare-earth (0001) surfaces exhibit a highly localized surface state near the Fermi edge. After the adsorption of hydrogen the surface state disappeared, and an additional sharp feature at about 4-eV binding energy was observed. For this latter d_{z^2}-like state the ratio of the radial matrix elements as well as the relative phase shifts were determined to be $R_p/R_f = 2.4 \pm 0.3$ and $\delta_f - \delta_p = 310° \pm 10°$, respectively using the possibility to rotate the electric-field vector continuously. [S0163-1829(98)10335-1]

In the description of the photoemission process, the determination of the differential cross section plays an important role. For a fixed spatial arrangement the angular distribution of photoelectrons can be deduced if the dipole matrix elements and the phase shifts of the outgoing photoelectron wave are known. One example for the determination of these values is the circular dichroism in the angular distribution of photoelectrons.[1] In this experimental technique the photoelectron intensity as a function of detection angle is compared for excitation with left and right circularly polarized light, respectively. The important parameters for the description of the intensity difference are the dipole matrix elements and the relative phase shifts.

The determination is usually carried out with a fixed polarization of the incoming light and a variation of the emission angle. A restriction of this type of experimental arrangement is given by the limited range of the detection angle being further reduced due to the refraction of the escaping photoelectrons at the electrostatic surface barrier. Measurements at a fixed detection angle with a rotating electrical field vector enables one to avoid this restriction due to the possibility to use the whole angle range of 180°, giving a significantly more accurate set of data.

Additionally, information on quantum-mechanical quantities are usually obtained with a more or less larger experimental or theoretical effort. Being in contrast, the theoretical description of the latter type of angle resolving photoemission experiments as well as the experimental procedure are relatively simple. This method is suitable to be carried out in a laboratory because it does not need a sophisticated experimental setup like synchrotron radiation sources. It may therefore play an important role for an understanding of the photoemission process.

Here we report on a method to provide information about the dipole matrix elements and phase shifts being essential for the theoretical description of the photoemission process in a relatively simple way and with a pronounced accuracy. This can be achieved by means of photoelectron spectroscopy with linearly polarized light using the ability of a continuous rotation of the electric-field vector. This method is exemplarily demonstrated at the system hydrogen on Gd(0001)/W(110), which possesses a pronounced d_{z^2}-like adsorbate induced state.

For the determination of the electronic structure, angle-resolving photoelectron spectroscopy was used. Photoelectrons were produced by linearly polarized vacuum ultraviolet radiation from a discharge lamp (Ne I resonance line $h\nu = 16.85$ eV) with a triple-reflection polarizer. The angle of the incoming photon beam was $\theta_{\mathrm{ph}} = 45°$ with respect to the surface normal. A cylindrical mirror analyzer with sector field (300-mm slit-to-slit distance) and high transmission served as the energy dispersing element with the additional angular resolution of the photoelectrons (acceptance cone $\pm 3°$). The overall energy resolution was set to about 300 meV. The experiment was performed in a μ-metal ultrahigh-vacuum chamber to provide magnetic shielding, and the base pressure was below 3×10^{-11} mbar. It is equipped with a combined low-energy-electron-diffraction Auger system for surface characterization. An *in situ* transfer between the ultraviolet photoemission spectroscopy stage and scanning tunneling microscopy (STM) enables to investigate the *same* sample in order to determine the topography.

A W(110) crystal served as a substrate for the growth of Gd films. It was cleaned by heating in oxygen and flashing up to 2600 K. The Gd films were deposited by means of an electron-beam evaporator using tungsten crucibles. The growth rate was typically set to 0.5 layer per minute. The preparation procedure was based on the investigations in Ref. 2. Smooth Gd(0001) films were prepared by evaporation of more than 30 ML, with the substrate held at room temperature, and subsequent annealing at 700 K for 2 min. The topography was checked by STM. During Gd deposition the pressure stayed below 3×10^{-10} mbar. The surface was exposed to hydrogen by a high-precision leak valve. The amount is characterized in Langmuir ($1\ \mathrm{L} = 10^{-6}$ torr s), and not corrected by the ion gauge correction factor.

Photoelectron spectra from the Gd(0001) surface, being exposed to 1-L hydrogen, are shown in Fig. 1. The spectra are taken at room temperature for different detection angles θ. A pronounced feature at a binding energy of about 4 eV appears. The energy width (full width at half maximum) of

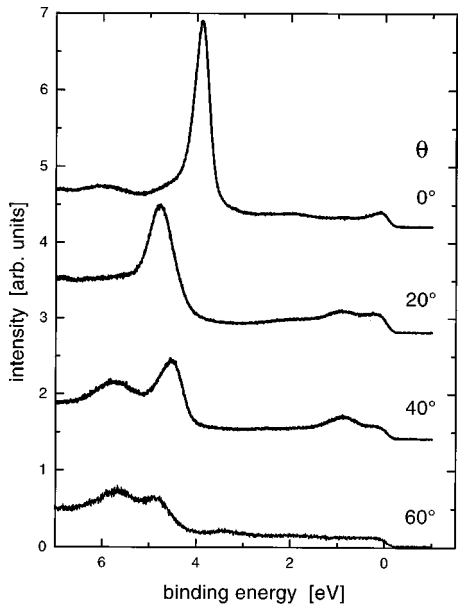

FIG. 1. Photoelectron spectra for different detection angles θ. Variations in binding energy, pointing to a dispersion, as well as in intensity, are present.

this H-induced state is equal to 0.4 eV and is similar to that of the surface state being energetically located near the Fermi edge,[3,4] indicating a well-ordered and clean hcp(0001) surface. This surface state is made responsible for extraordinary surface magnetic properties (e.g., Refs. 5 and 6). Offering adsorbates like hydrogen[7] and oxygen[8,9] suppresses the Gd surface state as well as the surface magnetization.

In Fig. 2(a), photoelectron spectra of the H-induced state are presented for different angles α of the **E**-field vector of the incoming linearly polarized photon beam with respect to the plane of incidence. $\alpha=90°$ denotes the case for *s*-polarized light. We find that at this angle the intensity of the H-induced state nearly vanishes, whereas the intensity is significantly enhanced for more *p*-polarized light.

The photoelectron intensity I (with the detector being at infinity) for atomic orbitals which are excited by a linearly polarized radiation source can be calculated via the differential cross section $d\sigma/d\Omega$[10]

$$I=\frac{d\sigma}{d\Omega}=\frac{4\pi}{3}\,\alpha a_0^2 h\nu|\langle\phi_{E_{\rm kin},\mathbf{k}}|\boldsymbol{\epsilon}\cdot\mathbf{r}|\phi_{n\ell x}\rangle|^2, \tag{1}$$

where α is the fine-structure constant, a_0 the Bohr radius, $\mathbf{k}$ the direction of the outgoing electron, $\boldsymbol{\epsilon}$ the polarization vector, and $\mathbf{r}$ the position vector at angles θ and ϕ. The initial real atomic orbital is given by

$$\phi_{n\ell x}=R_{n\ell}(r)\sum_m n(m)Y_{\ell m}(\theta,\phi), \tag{2}$$

where $Y_{\ell m}(\theta,\phi)$ is a spherical harmonic and $n(m)$ are the coefficients needed to form real orbitals such that ℓx is s, p_z, etc. The final state is written[11] as a partial-wave expansion

$$\phi_{E_{\rm kin},\mathbf{k}}=4\pi\sum_{\ell' m'} i^{\ell'}e^{-i\delta_{\ell'}}Y^*_{\ell',m'}(\theta_k,\phi_k)\times Y_{\ell',m'}(\theta,\phi)R_{E_{\rm kin},\ell'}. \tag{3}$$

The photoelectron intensity of the hydrogen-induced state was determined [cf. Fig. 2(a)] as a function of the vector potential of the incoming radiation, and is shown in Fig. 2(b) (open circles). The electric-field vector of the light was rotated by the angle α in the plane perpendicular to the direction of propagation. For $\alpha=0°$, the light is more *p* polarized, whereas for $\alpha=90°$ it is *s* polarized. The intensity exhibits maxima at 0° and 180°, respectively. A d_{z^2}-like orbital symmetry of this state was previously deduced by Li *et al.*[7] from the observation that the constant initial state spectra were the same for both the hydrogen-induced state and the Gd surface state. Using the equations above and dipole selection rules $\Delta\ell=\pm1$ and $\Delta m=\pm1,0$ the dipole matrix element for such a d_{z^2} initial state can be calculated to be

$$\begin{aligned}\langle\phi_{E_{\rm kin},\mathbf{k}}|\mathbf{e}\cdot\mathbf{r}|d_{z^2}\rangle=&\sqrt{8\pi}\{e^{i\delta_p}R_p[\sqrt{1/10}\,\sin\,\theta(\epsilon_x\cos\,\phi+\epsilon_y\sin\,\phi)-\epsilon_z\sqrt{2/5}\cos\,\theta]\\&+e^{i\delta_f}R_f\sqrt{9/40}[\sin\,\theta(5\cos^2\,\theta-1)(\epsilon_x\cos\,\phi+\epsilon_y\sin\,\phi)\\&+\epsilon_z(5\cos^3\,\theta-3\cos\,\theta)]\}.\end{aligned} \tag{4}$$

In normal emission ($\theta=0$) this expression is determined by ϵ_z being proportional to cos α. The intensity using a rotating electric-field vector is therefore $\propto\cos^2\alpha$ [cf. Eq. (1)]. This behavior is demonstrated by the solid line in Fig. 2(b), presenting a fit with a $\cos^2$ function.

Dispersion effects of the parallel momentum component $k_\parallel$ from the outgoing electron was investigated by rotating the sample with the radiation source and analyzer kept fixed in space. The photoelectron spectra for angles between $\theta=0°$ and 60° were already shown in Fig. 1. Whereas in normal emission the spectrum is dominated by the hydrogen-induced structure at about 4-eV binding energy, this feature loses intensity with increasing detection angle, and shifts in energy, directly pointing to a nonvanishing dispersion. For higher angles additional structures at 1- and 5.5-eV binding energy appear. The highly localized Gd surface state near E_F is nearly dispersionless. In contrast, the H-induced states possess different binding energies when varying the photoelectron detection angle θ. The $k_\parallel$ dispersion directly points to an overlap of the hydrogen wave functions within the overlayer, or hybridization with the Gd bulk bands.

The dipole matrix element contains the radial parts R_p and R_f as well as phase shifts δ_p and δ_f [see Eq. (4)]. In order to obtain information about these properties the photo-

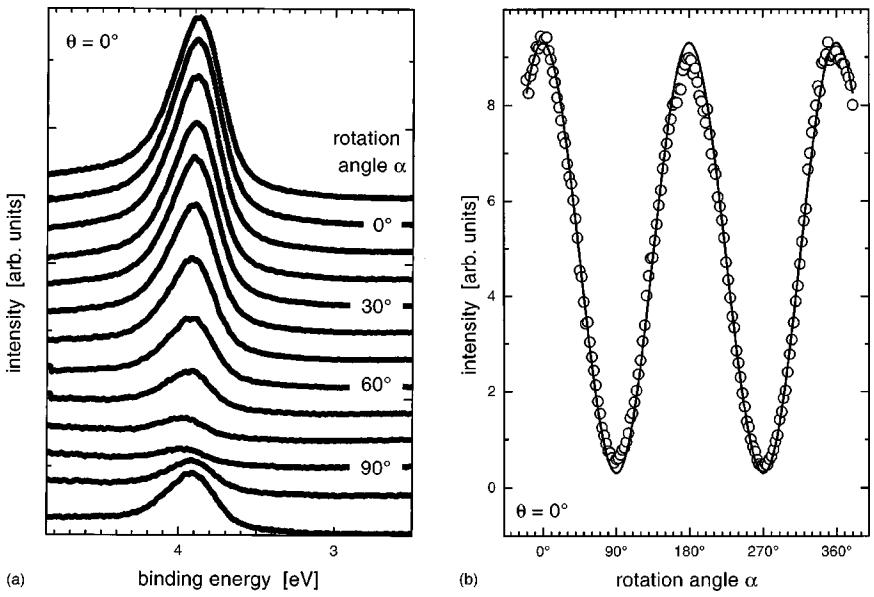

FIG. 2. (a) Photoelectron spectra (normal emission) for the hydrogen-induced structure as a function of the rotation angle α of the linear polarizer. (b) Photoemission intensities of the maximum for the H-induced feature at about 4-eV binding energy depending on the rotation angle α of the incoming linearly polarized radiation; the solid line represents a fit with $\cos^2$ function. The spectra were taken in normal emission.

electron intensities were determined at a fixed detection angle $\theta=45°$ as a function of the rotation of the **E**-field vector. The spectra in Fig. 3 are shown for special values of α at which the maximum and minimum intensities are reached for the peak 2 at 4.7 eV (4.0 eV in normal emission) with $\alpha=170°$ and 80° as well as for the feature 1 at 1 eV and structure 3 at 6 eV, with $\alpha=140°$ and 50°, respectively. The intensity values are summarized in Fig. 4 (♦: peak 1; ○: peak 2; •: peak 3). The curves for peaks 1 and 3 show the same shape, which may be caused by emission from orbitals with the same symmetry, but being different from the d_{z^2}-like state (peak 2). Equation (4) can be expressed in terms of quantities $X_{\ell\pm1,x}$:[10]

$$\langle \phi_{E_{\mathrm{kin}},\mathbf{k}} | \boldsymbol{\epsilon}\cdot\mathbf{r} | \phi_{n\ell x} \rangle = (-i)^{\ell-1}(e^{i\delta_{\ell-1}}X_{\ell-1,x}+e^{i\delta_{\ell+1}}X_{\ell+1,x}). \quad (5)$$

For this experimental geometry these X functions are given by

$$X_{\ell-1,x}=R[\sin\theta(\sin\alpha+\sqrt{1/2}\cos\alpha) - 2\cos\theta(\sin\alpha-\sqrt{1/2}\cos\alpha)], \quad (6)$$

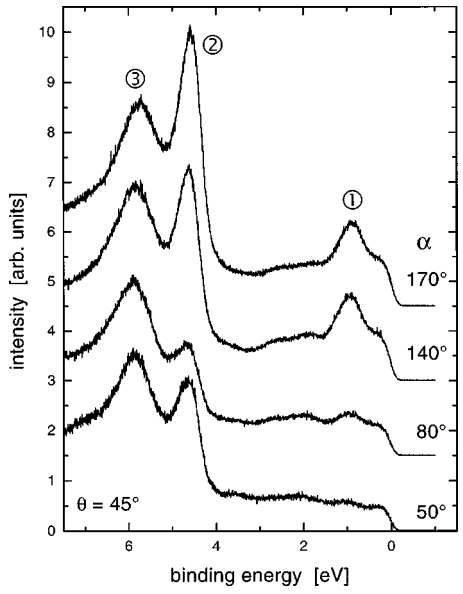

FIG. 3. Photoemission intensities at a fixed detection angle $\theta=45°$ for special values of the rotation angle α (see text).

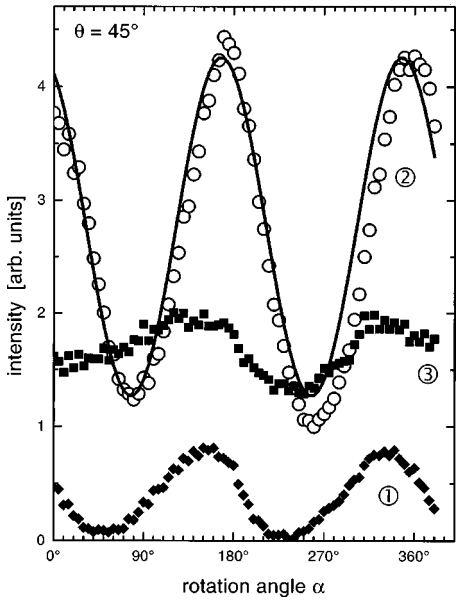

FIG. 4. Photoemission intensities of the maximum for the three peaks labeled in Fig. 3. The shapes of curves 1 and 3 are the same one, but different to that of curve 2. The solid line represents a fit as discussed in the text.

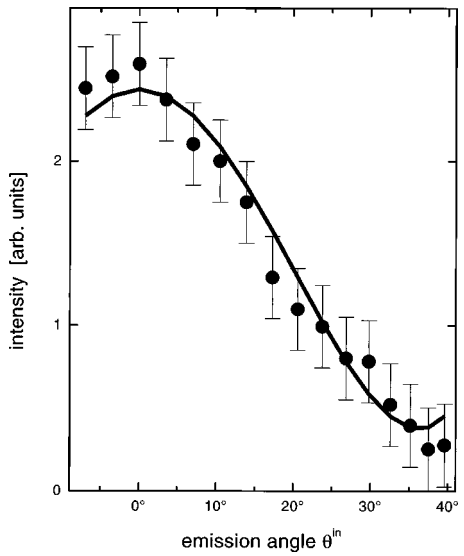

FIG. 5. Photoemission intensities as a function of the detection angle θ. The angle scale is given by the emission angle θ^{in} inside the surface barrier, which can be deduced from the detection angle taking into account the inner potential [Eq. (9)].

$$X_{\ell+1,x}=1.5[\sin\theta(5\cos^2\theta-1)(\sin\alpha+\sqrt{1/2}\cos\alpha)+\cos\theta(5\cos^2\theta-3)(\sin\alpha-\sqrt{1/2}\cos\alpha)] \tag{7}$$

using the simplification $R_f=1$ and $R=R_p/R_f$. The photoelectron intensity then is given by

$$I\propto X^2_{\ell+1,x}+X^2_{\ell-1,x}+2X^2_{\ell+1,x}X^2_{\ell-1,x}\cos(\delta_{\ell+1}-\delta_{\ell-1}). \tag{8}$$

However, the angle θ in these equations is not the detected one, as can be seen by the following consideration. In off-normal measurements ($\theta\neq 0$) the detection angle θ with the detector at infinity corresponds to a smaller one in or near the crystal. This effect is due to the refraction of an outgoing electron wave at the electrostatic surface barrier. When surmounting this barrier, the momentum parallel to the surface remains constant, the one perpendicular becomes reduced. This phenomenon results in an increased emission angle (with respect to the surface normal) outside the surface region. The inner, i.e., true, emission angle θ^{in} can be deduced from the outer, i.e., observed, angle $\theta^{\text{out}}=\theta$ using the relation[12,13]

$$\sqrt{E_{\text{kin}}-V_0}\,\sin\theta^{\text{in}}=\sqrt{E_{\text{kin}}}\,\sin\theta^{\text{out}}, \tag{9}$$

where E_{kin} is the kinetic energy of the photoelectron, and V_0 the inner potential being the difference in kinetic-energy inside and outside the surface barrier. The binding energy of the hydrogen-induced structure corresponds to a kinetic energy of about 10 eV. Assuming a typical value for the inner potential of $V_0=-10$ eV the maximum value for the detection angle $\theta^{\text{out}}=90°$ corresponds to an inner angle $\theta^{\text{in}}=45°$; i.e., the ''observable'' angle range is limited to this value of 45°. The detection angle $\theta=45°$ (cf. Fig. 3) therefore corresponds to an inner angle $\theta^{\text{in}}=30°$ which must be used in Eqs. (6) and (7). A least-squares fit for the d_{z^2}-like hydrogen-induced structure (curve 2 in Fig. 4) results in $R=2.4\pm0.3$ and $\delta_f-\delta_p=310°\pm10°$. In order to verify these values, the intensity of the same feature was determined as a function of the detection angle (cf. Fig. 1). These values are presented in Fig. 5. Calculating the X function for this experimental geometry and inserting $R=2.4$ and $\delta_f-\delta_p=310°$ into the equation results in the function which is shown as a solid line in Fig. 5. There is a good agreement within the experimental error, corroborating the findings for the ratio of the radial matrix elements and the relative phase shift.

In summary we have determined the electronic structure of hydrogen on Gd(0001). By means of photoelectron spectroscopy with linearly polarized radiation in combination with the possibility to rotate the electric-field vector of the incoming photon beam, the ratio of the radial matrix elements $R=R_p/R_f$ as well as the relative phase shift $\delta_f-\delta_p$ were determined for the wave function of the hydrogen state with a binding energy of about 4 eV to be $R=2.4\pm0.3$ and $\delta_f-\delta_p=310°\pm10°$. The measurements of our investigation at a fixed detection angle with a rotating electric-field vector can be carried out over the *whole angle range* of 180°, giving a significantly more accurate set of data in comparison to measurements with a fixed linear polarization and a varying emission angle.

We thank G. H. Fecher for a stimulating discussion, and acknowledge financial support by the DFG through Grant No. Wi 1277/3-2.

[1] C. Westphal *et al.*, Phys. Rev. Lett. **63**, 151 (1989).
[2] A. Aspelmeier, F. Gerhardter, and K. Baberschke, J. Magn. Magn. Mater. **132**, 22 (1994).
[3] B. Kim *et al.*, Phys. Rev. Lett. **68**, 1931 (1992).
[4] G. A. Mulhollan, K. Garrison, and J. L. Erskine, Phys. Rev. Lett. **69**, 3240 (1992).
[5] D. Weller *et al.*, Phys. Rev. Lett. **54**, 1555 (1985).
[6] H. Tang *et al.*, Phys. Rev. Lett. **71**, 444 (1993).
[7] D. Li *et al.*, Phys. Rev. B **48**, 5612 (1993).
[8] E. Vescovo *et al.*, Phys. Rev. B **47**, 13 899 (1993).
[9] D. N. McIlroy *et al.*, Phys. Rev. Lett. **76**, 2802 (1996).
[10] S. M. Goldberg, C. S. Fadley, and S. Kono, J. Electron Spectrosc. Relat. Phenom. **21**, 285 (1981).
[11] J. W. Gadzuk, Phys. Rev. B **12**, 5608 (1975).
[12] K. Horn, A. M. Bradshaw, and K. Jacobi, Surf. Sci. **72**, 719 (1978).
[13] M. Scheffler, K. Kambe, and F. Forstmann, Solid State Commun. **25**, 93 (1978).